Proceedings of the 6th JFPS International
Symposium on Fluid Power, TSUKUBA 2005
November 7-10, 2005

CHARACTERISTICS OF THE COMPRESSIBLE FLOW BETWEEN TWO PARALLEL DISKS

Hiroyuki SATO*, Koji TAKAHASHI**, Keigo OHTANI***, Shigeru IKEO****

*Development Department, Technical Center, SMC Corporation
4-2-2, Kinunodai, Yawara-mura, Tsukuba-gun, Ibaraki 300-2493, Japan
(E-mail: hiroyuki_sato@smcjpn.co.jp)
**Professor Emeritus, Sophia University
4-23-9 Hiyoshicho, Kokubunji, Tokyo 185-0032, Japan
***Data Processing Department, Suzuki Motor Corporation
1300 Takatsukacho, Hamamatsu-shi, Shizuoka 432-8611, Japan
****Professor, Department of Mechanical Engineering, Sophia University
7-1 Kioicho, Chiyoda-ku, Tokyo 102-8554, Japan

ABSTRACT

Compressible flows between two parallel disks are frequently encountered in fluid power components such as pneumatic statistical bearings, pneumatic nozzle-flapper valves and pneumatic valves. Such flows are difficult to solve theoretically because both viscous and compressible effects exist. In the present study, a theory is developed to predict the flow characteristics, assuming that the flow is one dimensional and steady. Experiments are performed, and their results agree fairly well with theoretical results.

KEY WORDS

Viscous compressible flow, Flow characteristics, Critical pressure ratio, choked flow rate

NOMENCLATURE

A : flow sectional area $=2\pi rh$
b : critical pressure ratio
c_p : specific heat at constant pressure
d_i : valve seat hole diameter $=2r_i$
f : friction factor=0.0026
h : gap clearance
k : specific heat ratio=1.40
LL : lap length (see Figure 1)
M : Mach number
p : absolute pressure
R : gas constant=287 J/(kg.K)
r : radial coordinate
T_0 : stagnation temperature, constant for an adiabatic flow
T : absolute temperature
V : mean velocity at a section
w : mass flow rate
ρ : fluid density

Subscript
e : outer edge of the gap
i : inner edge of the gap
0 : upstream condition
* : condition at the choked flow

INTRODUCTION

Flows between two parallel disks are frequently seen in fluid power components such as statistical bearings, nozzle-flapper valves and seat valves. Although many theoretical papers [1] have been published for incompressible flows, those related to compressible flows are not so many, because for such flows both viscous and compressible effects should be taken into consideration.

Mori [2] analyzed an unstable phenomenon named whirl which occurs in a gas bearing. Ogami [3] analyzed a one-dimensional viscous compressible flow by numerical method. Kamiyama and Yamamoto [4] numerically investigated a compressible flow in aerostatic journal bearing. Kobayashi [5] investigated the stability of gas-lubricated journal bearings experimentally and numerically.

In the present study, the authors assumed the flow between two parallel disks to be one-dimensional and steady and developed a theory to solve the flow. Experiments were performed, and the comparison between theoretical and experimental results showed that the theory can predict the flow characteristics.

THEORY

The flow between two disks as shown in Figure 1 is to be analyzed [6].

The equation of state for an ideal fluid is

$$p=\rho RT \tag{1}$$

Mach number is

$$M^2=V^2/(kRT) \tag{2}$$

The energy equation for adiabatic flow is

$$c_p T + \frac{V^2}{2} = c_p T_0 \tag{3}$$

The continuity equation is

$$w=A\rho V=2\pi rh\rho V \tag{4}$$

Applying the equation of motion for steady flow in the radial direction, we have

$$VdV = -\frac{dp}{\rho} - \frac{\tau}{\rho}\frac{dA_w}{A} \tag{5}$$

where τ is the wall shear stress and dA_w is the wetted area on which τ is exerted.

Provided that the friction losses between two disks are similar to those in a circular tube, friction factor f is defined by

$$f = \frac{\tau}{\rho V^2/2} \tag{6}$$

Differentiating Eqs.(1), (2), (3) and (4), and combining these equations, Eqs.(5) and (6), we finally obtain the following:

$$\frac{dp}{p} + \frac{dr}{r} = -\frac{1+(k-1)M^2}{2\left(1+\frac{k-1}{2}M^2\right)}\frac{dM^2}{M^2} \tag{7}$$

and

$$\frac{1-M^2}{M^2\left(1+\frac{k-1}{2}M^2\right)}dM^2 = 2\left(\frac{fkM^2}{h} - \frac{1}{r}\right)dr \tag{8}$$

Generally speaking, Eq.(8) may be difficult to be solved. Friction factor f, however, has normally a small value and the effect of M^2 in the first term in the parenthesis on the right-hand side will be small. Accordingly, assuming that M^2 is constant,

$$M^2 \approx M_{av}{}^2 = \left(M_i{}^2 + M_e{}^2\right)/2 = \text{const} \tag{9}$$

Then, Eq.(8) can be integrated from r_i to r_e to obtain the following:

$$\frac{r_e}{r_i}\frac{G(M_i)}{G(M_e)} = \alpha \tag{10}$$

where

$$G(M) = \frac{1}{M}\left(1+\frac{k-1}{2}M^2\right)^{\frac{k+1}{2(k-1)}} \tag{11}$$

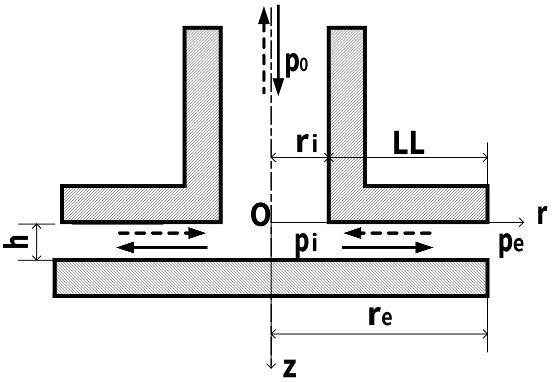

Figure 1 Flow between two parallel disks

and

$$\alpha = \exp\left[\frac{fkM_{av}{}^2(r_e-r_i)}{h}\right] \approx 1 + \frac{fkM_{av}{}^2(r_e-r_i)}{h} \tag{12}$$

Outward flow

Integrating Eq.(7), we get

$$\frac{p_e}{p_i}=\frac{r_i}{r_e}\frac{M_i}{M_e}\sqrt{\frac{1+\frac{k-1}{2}{M_i}^2}{1+\frac{k-1}{2}{M_e}^2}}=\frac{r_i}{r_e}\frac{H(M_i)}{H(M_e)} \quad (13)$$

where

$$H(M)=M\sqrt{1+\frac{k-1}{2}M^2} \quad (14)$$

In an outward flow, pressure p_e at the outer edge divided by stagnation pressure p_0 upstream is usually taken as pressure ratio for outward flow.

The following formula holds for isentropic change:

$$\frac{p_0}{p_i}=\left(\frac{\rho_0}{\rho_i}\right)^k=\left(\frac{T_0}{T_i}\right)^{\frac{k}{k-1}} \quad (15)$$

Combining Eqs.(2), (3) and (15) we have

$$p_i=\frac{p_0}{\left(1+\frac{k-1}{2}{M_i}^2\right)^{\frac{k}{k-1}}} \quad (16)$$

By substituting p_i in Eq.(16) into Eq.(13) and using Eq.(10), the pressure ratio p_0/p_i is obtained as follows:

$$\frac{p_e}{p_0}=\frac{r_i}{r_e}\frac{1}{G(M_i)H(M_e)}=\frac{1}{\alpha G(M_e)H(M_e)}=\frac{1}{\alpha\left(1+\frac{k-1}{2}{M_e}^2\right)^{\frac{k}{k-1}}} \quad (17)$$

When substituting any Mach number M_i at the inner edge and Mach number M_e obtained from Eq.(10) into Eq.(17), the pressure ratio p_e/p_0 corresponding to M_i can be calculated.

Next, mass flow rate w is to be obtained. Substituting Eqs.(1), (2), (16) and (15) into Eq.(4) we get

$$w(M_i)=2\pi r_i h\sqrt{\frac{k}{R}}\frac{p_0}{\sqrt{T_0}}\frac{M_i}{\left(1+\frac{k-1}{2}{M_i}^2\right)^{\frac{k+1}{2(k-1)}}}=2\pi r_i h\sqrt{\frac{k}{R}}\frac{p_0}{\sqrt{T_0}}\frac{1}{G(M_i)} \quad (18)$$

Choked flow rate w^* is

$$w^*=2\pi r_i h\sqrt{\frac{k}{R}}\frac{p_0}{\sqrt{T_0}}\frac{1}{G(1)} \quad (18')$$

When Mach number M_i at the inner end is unity, Eq.(10) is rearranged as

$$\alpha(1,\, r_e)G(M_{ec})-\frac{r_e}{r_i}G(1)=0 \quad (19)$$

where M_{ec} is the Mach number at the outer end corresponding to M_i=1.

Substituting the value of M_{ec} into Eq.(17), critical pressure ratio b is expressed as

$$b=\frac{1}{\alpha}\frac{1}{\left(1+\frac{k-1}{2}{M_{ec}}^2\right)^{\frac{k}{k-1}}} \quad (20)$$

Inward flow

Consider an inward flow in which the flow is reversed. In this case subscript e denotes upstream conditions, and subscript i downstream ones in Figure 1. Since most equations derived for an outward flow can be applied as well, we will describe here only those equations which need modification. It should be noted that velocity V is negative, so that shear stress τ and friction factor f are negative. Consequently α in Eq. (10) should be replaced by $1/\alpha$

$$\frac{r_i}{r_e}\frac{G(M_e)}{G(M_i)}=\alpha \quad (21)$$

Giving any value of M_e into Eq.(21), we can get M_i.

Equation (16) is modified as follows:

$$p_e=\frac{p_0}{\left(1+\frac{k-1}{2}{M_e}^2\right)^{\frac{k}{k-1}}} \quad (22)$$

In an inward flow, pressure p_i at the inner edge divided by stagnation pressure p_0 upstream is usually taken as pressure ratio for inward flow, which is expressed by

$$\frac{p_i}{p_0}=\frac{r_e}{r_i}\frac{1}{G(M_e)H(M_i)} \quad (23)$$

Substitution of Eq.(21) into Eq.(23) yields

$$\frac{p_i}{p_0} = \frac{1}{\alpha\left(1+\frac{k-1}{2}M_i^{\,2}\right)^{\frac{k}{k-1}}} \qquad (24)$$

When substituting any Mach number M_e at the outer edge and Mach number M_i obtained from Eq.(21) into Eq.(17), the pressure ratio p_i/p_0 corresponding to M_e can be calculated.
Using Eq.(21) mass flow w is expressed by

$$w = 2\pi r_e h\sqrt{\frac{k}{R}}\frac{p_0}{\sqrt{T_0}}\frac{1}{\alpha G(M_i)} \qquad (25)$$

Choked flow rate w^* is

$$w^* = 2\pi r_e h\sqrt{\frac{k}{R}}\frac{p_0}{\sqrt{T_0}}\frac{1}{G(1)}\frac{1}{\alpha(M_e, r_i)} \qquad (25')$$

When Mach number M_i at the inner end is unity, Eq.(21) is rearranged as

$$\frac{G(M_{ec})}{\alpha} - \frac{r_e}{r_i}G(1) = 0 \qquad (26)$$

where M_{ec} is the Mach number at the outer end corresponding to M_i=1.
Substituting the value of M_{ec} into Eq.(24), critical pressure ratio b is expressed as

$$b = \frac{1}{\alpha}\left(\frac{2}{k+1}\right)^{\frac{k}{k-1}} \qquad (27)$$

When there is no friction loss, α becomes unity, and b=0.528, which coincides with the value for the isentropic flow in a convergent nozzle.

EXPERIMENT

Figure 2 shows the test valve used. In an outward flow compressed air was fed from port A, and in an inward flow from port B.
The supply pressure of air was kept 500 kPa abs, and air temperature was 290 K during experiments. The downstream pressure (p_e for an outward flow and p_i for an inward flow) was adjusted with a throttle valve placed downstream of the test valve.
In Figure 1, actual dimensions are as follows:
Outer radius r_e=10 mm,
Valve seat hole diameter d_i=5 and 10 mm,
Lap length LL=1, 3 and 5 mm.

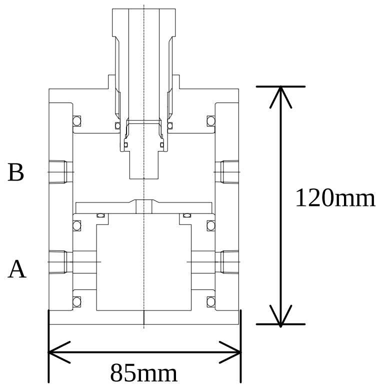

Figure 2 Test valve

RESULTS

Flow characteristic

Figure 3(a) shows an example of the comparison of the calculated results with the experimental ones for an

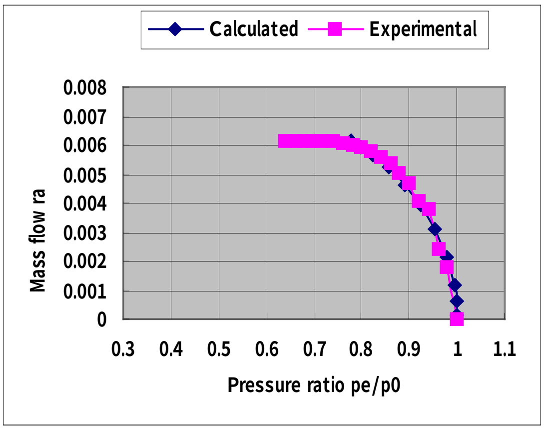

(a) Outward flow

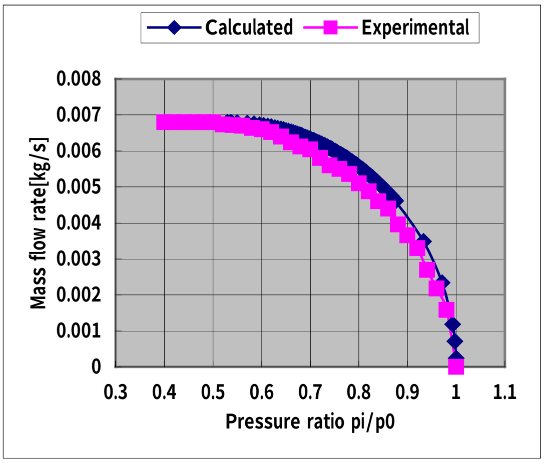

(b) Inward flow

Figure 3 Comparison between theory and experiment, d_i =10 mm, LL=5 mm outward flow with some modification in lap length explained later, and Figure 3(b) for an inward flow.

The calculated results agree well with the experimental ones for inward flows. The values of critical pressure ratio are close to 0.528, the value of critical pressure ratio for isentropic flow in a convergent nozzle.

In an outward flow, however, calculated results did not agree well with experimental ones. And the calculated results deviate from the experimental ones as approaching choke flow. It can be deduced that flow separation might occur at the inner end. It would be necessary to estimate the lap length smaller than the real size. In Figure 3(a), LL was set to 0.9 mm instead of 5 mm in calculation, the difference in LL is considered to be the flow separation. After this modification, calculated results agree fairly well with experimental ones, as shown in Figure 3(a).

Figure 4 shows that for the same gap width choked flow rate w^* for an outward flow is less than that for an inward flow.

As can be seen from Figures 5(a) and 5(b), critical pressure ratios for outward flows are greater than those for inward flows.

Effect of viscosity

Throughout the experiment, gap width h was between 0.1 and 0.3 mm. For such widths, α in Eq. (12) is approximately unity, and the viscous effect of air can be neglected. For smaller gap width, however, it would be necessary to take into consideration the effect of friction.

Effect of lap length

Figure 5(a) shows the experimental results of the effect of lap length on critical pressure ratio for outward flows, and Figure 5(b) for inward flows. In theory, the lap length only affects friction, which is very small in the range of experiment, the results for inward flows are reasonable.

In outward flows, however, critical pressure ratio increases with an increase in lap length.

Critical pressure ratio vs. mass flow rate

Figures 6 show the relations between critical pressure ratio b and choked mass flow rate w^*. According to the theory, as can be seen from Eqs.(20) and (27), values of critical pressure ratio are independent of choked flow rate in frictionless flows (α=1).

In experiment, choked mass flow rate w^* gives little effect on b for both outward and inward flows as shown in Figures 6, and the theory agrees to the experimental results in the range of the experiment. More experiments with larger flow rates would be necessary, however, to confirm the validity of the theory.

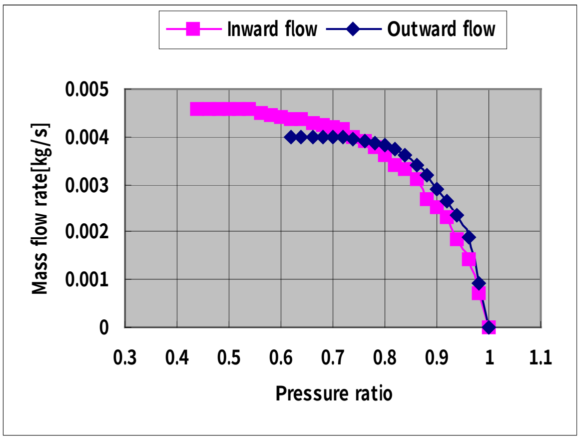

Figure 4 Comparison between outward and inward flows, d_i=5 mm, h=0.22 mm

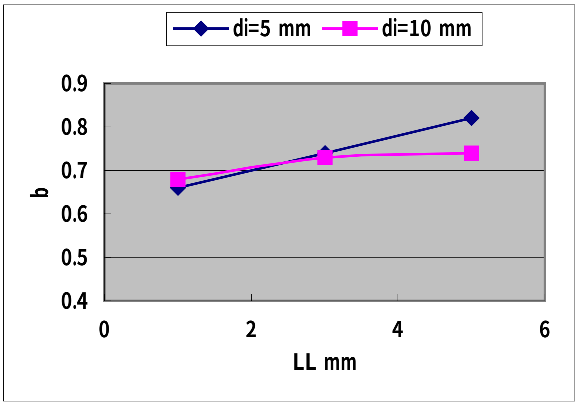

(a) Outward flow

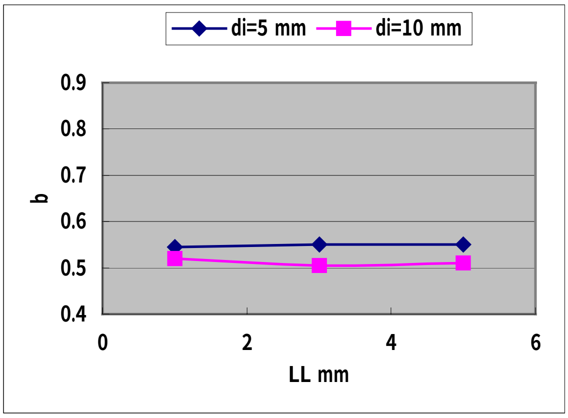

(b) Inward flow

Figure 5 Effect of lap length

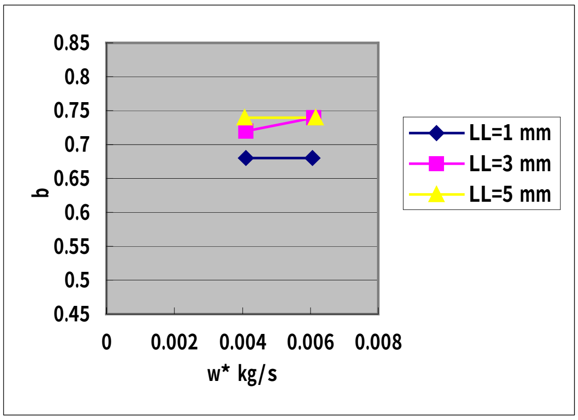

(a) Outward flow

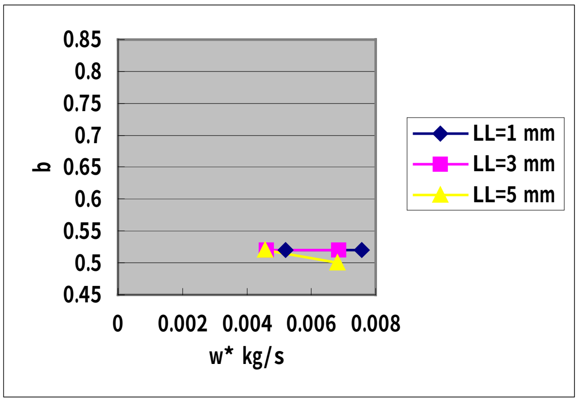

(b) Inward flow

Figure 6 Relation between critical pressure ratio and choked mass flow rate, d_i=10 mm

CONCLUDING REMARKS

A theory is developed for flow characteristics between two parallel disks, and its validity is confirmed by the comparison with experimental results. In regard to outward flows, however, some discordance between theory and experiment is observed.

Consequently, the following conclusions are drawn:

1) In inward flows, flow characteristics can be predicted from the theory. The value of critical ratio is close to that of convergent nozzle flow;

2) In outward flows, some modification is necessary to apply the theory to flow characteristics, i.e., the lap length in lap length should be taken smaller than real size.

This is considered to result from the separation at the inner edge of the gap;

3) For the same gap width, the choked flow rate for outward flows is less than that for inward flows;

4) Critical pressure ratio for outward flows is generally larger than that for inward flows;

5) Friction losses through the gap little affect the values of w^* and b in the range of this study, i.e., gap widths larger than 0.1 mm. If the gap width were more reduced, however, the frictional effect would appear;

6) In outward flows, an increase in lap length increases critical pressure ratio, while in inward flows lap length little affects the value.

ACKNOWLEDGMENT

The authors would like to express their deepest appreciation to Messrs. N. Oneyama, H. Zhang and M. Senoo, Technical Center of SMC Corporation, for their kind help and advice in conducting this study.

REFERENCES

1. e.g., Ishizawa, S., Watanabe, T. and Takahashi, K., Unsteady Viscous Flow between Parallel Disks with a Time-Varying Gap Width and a Central Fluid Source, Trans. ASME, J. Fluid Eng. Vol.109, (1987), p.394
2. Mori, A., On the Whirl Instability in Gas-Bearings (In Japanese), Lubrication, Vol.20, No.7, (1975), p.481
3. Ogami et al, Numerical Simulation of One-Dimensional Viscous Compressible Fluid Motion Using particle method (In Japanese), Trans. JSME, Vol.62, No.604, (1996), p.4084
4. Kamiyama, T. and Yamamoto, M., Numerical Investigation of Compressible Flow within Aerostatic Journal Bearing (In Japanese), Trans. JSME, Ser. B, Vol.65, No.629, (1999), p.144
5. Kobayashi, T., Stability of Axially-Grooved Self-Acting Gas-Lubricated Journal Bearings (In Japanese), Trans. JSME, Ser. C, Vol.65, No.629, (1999), p.330
6. e.g., Shapiro, A. H.: The Dynamics and Thermodynamics of Compressible Fluid Flow, Vol. 1, (1953), Ronald Press, p. 80